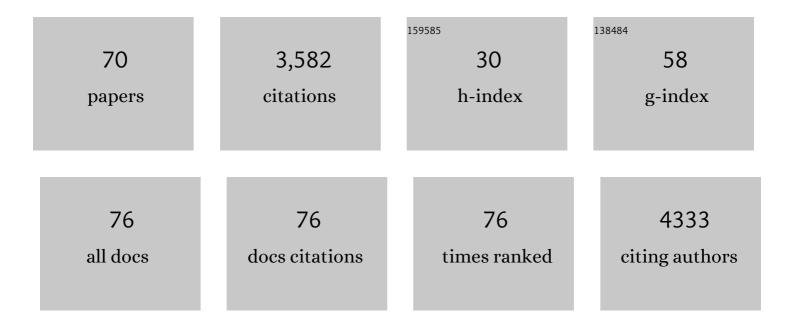
Andrei José Petrescu

List of Publications by Year in descending order

Source: https://exaly.com/author-pdf/4539682/publications.pdf Version: 2024-02-01



#	Article	IF	CITATIONS
1	Conformational Studies of Oligosaccharides and Glycopeptides:  Complementarity of NMR, X-ray Crystallography, and Molecular Modelling. Chemical Reviews, 2002, 102, 371-386.	47.7	400
2	Statistical analysis of the protein environment of N-glycosylation sites: implications for occupancy, structure, and folding. Glycobiology, 2003, 14, 103-114.	2.5	391
3	Coiled-Coil Domain-Dependent Homodimerization of Intracellular Barley Immune Receptors Defines a Minimal Functional Module for Triggering Cell Death. Cell Host and Microbe, 2011, 9, 187-199.	11.0	269
4	Harmonicity in slow protein dynamics. Chemical Physics, 2000, 261, 25-37.	1.9	197
5	Nucleocytoplasmic Distribution Is Required for Activation of Resistance by the Potato NB-LRR Receptor Rx1 and Is Balanced by Its Functional Domains. Plant Cell, 2011, 22, 4195-4215.	6.6	140
6	A statistical analysis of N- and O-glycan linkage conformations from crystallographic data. Glycobiology, 1999, 9, 343-352.	2.5	125
7	Mutations at Critical N-Glycosylation Sites Reduce Tyrosinase Activity by Altering Folding and Quality Control. Journal of Biological Chemistry, 2000, 275, 8169-8175.	3.4	113
8	A Secreted SPRY Domain-Containing Protein (SPRYSEC) from the Plant-Parasitic Nematode <i>Globodera rostochiensis</i> Interacts with a CC-NB-LRR Protein from a Susceptible Tomato. Molecular Plant-Microbe Interactions, 2009, 22, 330-340.	2.6	109
9	A Caenorhabditis elegans Wild Type Defies the Temperature–Size Rule Owing to a Single Nucleotide Polymorphism in tra-3. PLoS Genetics, 2007, 3, e34.	3.5	104
10	Transposon molecular domestication and the evolution of the RAG recombinase. Nature, 2019, 569, 79-84.	27.8	100
11	The solution NMR structure of glucosylated N-glycans involved in the early stages of glycoprotein biosynthesis and folding. EMBO Journal, 1997, 16, 4302-4310.	7.8	91
12	In Planta Secretion of a Calreticulin by Migratory and Sedentary Stages of Root-Knot Nematode. Molecular Plant-Microbe Interactions, 2005, 18, 1277-1284.	2.6	91
13	Tyrosinase Folding and Copper Loading in Vivo: A Crucial Role for Calnexin and α-Glucosidase II. Biochemical and Biophysical Research Communications, 1999, 261, 720-725.	2.1	82
14	Structural aspects of glycomes with a focus on N-glycosylation and glycoprotein folding. Current Opinion in Structural Biology, 2006, 16, 600-607.	5.7	79
15	Inhibition of N-Glycan Processing in B16 Melanoma Cells Results in Inactivation of Tyrosinase but Does Not Prevent Its Transport to the Melanosome. Journal of Biological Chemistry, 1997, 272, 15796-15803.	3.4	76
16	Structural Determinants at the Interface of the ARC2 and Leucine-Rich Repeat Domains Control the Activation of the Plant Immune Receptors Rx1 and Gpa2 Â Â Â. Plant Physiology, 2013, 162, 1510-1528.	4.8	73
17	Radially Softening Diffusive Motions in a Globular Protein. Biophysical Journal, 2001, 81, 1666-1676.	0.5	72
18	Mutations in dopachrome tautomerase (Dct) affect eumelanin/pheomelanin synthesis, but do not affect intracellular trafficking of the mutant protein. Biochemical Journal, 2005, 391, 249-259.	3.7	66

#	Article	IF	CITATIONS
19	Origin, distribution and 3D-modeling of Gr-EXPB1, an expansin from the potato cyst nematodeGlobodera rostochiensis. FEBS Letters, 2005, 579, 2451-2457.	2.8	56
20	Tyrosinase and Glycoprotein Folding: Roles of Chaperones That Recognize Glycansâ€. Biochemistry, 2000, 39, 5229-5237.	2.5	53
21	Genome-wide functional analyses of plant coiled–coil NLR-type pathogen receptors reveal essential roles of their N-terminal domain in oligomerization, networking, and immunity. PLoS Biology, 2018, 16, e2005821.	5.6	52
22	Ancient diversity of splicing motifs and protein surfaces in the wild emmer wheat (<i>Triticum) Tj ETQq0 0 0 rgB Pathology, 2012, 13, 276-287.</i>	T /Overlocl 4.2	k 10 Tf 50 62 45
23	Protein specific N-glycosylation of tyrosinase and tyrosinase-related protein-1 in B16 mouse melanoma cells. Biochemical Journal, 1999, 344, 659-665.	3.7	42
24	Cell death triggering and effector recognition by Swâ€5 SDâ€CNL proteins from resistant and susceptible to a source to spotted wilt virus (i>. Molecular Plant Pathology, 2016, 17, 1442-1454.	4.2	42
25	N-Glycosylation Processing and Glycoprotein Foldingâ^'Lessons from the Tyrosinase-Related Proteins. Chemical Reviews, 2000, 100, 4697-4712.	47.7	41
26	An LRR/Malectin Receptor-Like Kinase Mediates Resistance to Non-adapted and Adapted Powdery Mildew Fungi in Barley and Wheat. Frontiers in Plant Science, 2016, 7, 1836.	3.6	39
27	Structural and functional characterization of a novel, host penetration-related pectate lyase from the potato cyst nematode Clobodera rostochiensis. Molecular Plant Pathology, 2007, 8, 293-305.	4.2	37
28	Random mutagenesis of the nucleotideâ€binding domain of <scp>NRC</scp> 1 (<scp>NB</scp> â€ <scp>LRR</scp> Required for Hypersensitive Responseâ€Associated Cell Deathâ€1), a downstream signalling nucleotideâ€binding, leucineâ€rich repeat (<scp>NB</scp> â€ <scp>LRR</scp>) protein, identifies gainâ€ofâ€function mutations in the nucleotideâ€binding pocket. New Phytologist, 2015, 208,	7.3	37
29	210-223. SPRYSEC Effectors: A Versatile Protein-Binding Platform to Disrupt Plant Innate Immunity. Frontiers in Plant Science, 2016, 7, 1575.	3.6	37
30	Tyrosinase Degradation Is Prevented when EDEM1 Lacks the Intrinsically Disordered Region. PLoS ONE, 2012, 7, e42998.	2.5	34
31	Small-angle neutron scattering by a strongly denatured protein: analysis using random polymer theory. Biophysical Journal, 1997, 72, 335-342.	0.5	33
32	LRRpredictor—A New LRR Motif Detection Method for Irregular Motifs of Plant NLR Proteins Using an Ensemble of Classifiers. Genes, 2020, 11, 286.	2.4	33
33	An N-Linked Glycan Modulates the Interaction between the CD1d Heavy Chain and β2-Microglobulin. Journal of Biological Chemistry, 2006, 281, 40369-40378.	3.4	28
34	Excluded volume in the configurational distribution of a stronglyâ€denatured protein. Protein Science, 1998, 7, 1396-1403.	7.6	27
35	RAG and HMGB1 create a large bend in the 23RSS in the V(D)J recombination synaptic complexes. Nucleic Acids Research, 2013, 41, 2437-2454.	14.5	23
36	Roles of the C-terminal domains of topoisomerase Ilα and topoisomerase Ilβ in regulation of the decatenation checkpoint. Nucleic Acids Research, 2017, 45, 5995-6010.	14.5	23

#	Article	IF	CITATIONS
37	Protein specific N-glycosylation of tyrosinase and tyrosinase-related protein-1 in B16 mouse melanoma cells. Biochemical Journal, 1999, 344, 659.	3.7	20
38	Three-Dimensional Modeling and Diversity Analysis Reveals Distinct AVR Recognition Sites and Evolutionary Pathways in Wild and Domesticated Wheat Pm3 R Genes. Molecular Plant-Microbe Interactions, 2014, 27, 835-845.	2.6	19
39	Identification of RAG-like transposons in protostomes suggests their ancient bilaterian origin. Mobile DNA, 2020, 11, 17.	3.6	19
40	C-Terminus Glycans with Critical Functional Role in the Maturation of Secretory Glycoproteins. PLoS ONE, 2011, 6, e19979.	2.5	19
41	Mapping and Quantitation of the Interaction between the Recombination Activating Gene Proteins RAG1 and RAG2. Journal of Biological Chemistry, 2015, 290, 11802-11817.	3.4	18
42	Heavy metal accumulation by Saccharomyces cerevisiae cells armed with metal binding hexapeptides targeted to the inner face of the plasma membrane. Applied Microbiology and Biotechnology, 2017, 101, 5749-5763.	3.6	18
43	Distinct Roles of Non-Overlapping Surface Regions of the Coiled-Coil Domain in the Potato Immune Receptor Rx1. Plant Physiology, 2018, 178, 1310-1331.	4.8	18
44	Structure–function analysis of ZAR1 immune receptor reveals key molecular interactions for activity. Plant Journal, 2020, 101, 352-370.	5.7	18
45	Change in backbone torsion angle distribution on protein folding. Protein Science, 2000, 9, 1129-1136.	7.6	12
46	Interface Analysis of the Complex between ERK2 and PTP-SL. PLoS ONE, 2009, 4, e5432.	2.5	12
47	Identification of an unusually sulfated tetrasaccharide chondroitin/dermatan motif in mouse brain by combining chipâ€nanoelectrospray multistage <scp>MS</scp> ² â€ <scp>MS</scp> ⁴ and high resolution <scp>MS</scp> . Electrophoresis, 2013, 34, 1581-1592.	2.4	12
48	The architecture of the 12RSS in V(D)J recombination signal and synaptic complexes. Nucleic Acids Research, 2015, 43, 917-931.	14.5	11
49	Clonal lineage of high grade serous ovarian cancer in a patient with neurofibromatosis type 1. Gynecologic Oncology Reports, 2018, 23, 41-44.	0.6	11
50	Collective dynamics of a photosynthetic protein probed by neutron spin-echo spectroscopy and molecular dynamics simulation. Physica B: Condensed Matter, 2000, 276-278, 514-515.	2.7	10
51	Gangliosidome of human anencephaly: A high resolution multistage mass spectrometry study. Biochimie, 2019, 163, 142-151.	2.6	9
52	Immunoaffinity Chromatography on Antibodies Immobilized on Nitrocellulose Powder. Analytical Biochemistry, 1995, 229, 299-303.	2.4	8
53	Evaluation of a neural networks QSAR method based on ligand representation using substituent descriptors. Journal of Molecular Graphics and Modelling, 2006, 25, 37-45.	2.4	8
54	Profiling Optimal Conditions for Capturing EDEM Proteins Complexes in Melanoma Using Mass Spectrometry. Advances in Experimental Medicine and Biology, 2019, 1140, 155-167.	1.6	8

#	Article	IF	CITATIONS
55	Inhibition of N-glycan processing modulates the network of EDEM3 interactors. Biochemical and Biophysical Research Communications, 2017, 486, 978-984.	2.1	7
56	Human caudate nucleus exhibits a highly complex ganglioside pattern as revealed by high-resolution multistage Orbitrap MS. Journal of Carbohydrate Chemistry, 2019, 38, 531-551.	1.1	7
57	Affinity Proteomics and Deglycoproteomics Uncover Novel EDEM2 Endogenous Substrates and an Integrative ERAD Network. Molecular and Cellular Proteomics, 2021, 20, 100125.	3.8	7
58	EDEM3 Domains Cooperate to Perform Its Overall Cell Functioning. International Journal of Molecular Sciences, 2021, 22, 2172.	4.1	7
59	Robosample: A rigid-body molecular simulation program based on robot mechanics. Biochimica Et Biophysica Acta - General Subjects, 2020, 1864, 129616.	2.4	5
60	Tyrosine 656 in topoisomerase Ill^2 is important for the catalytic activity of the enzyme: Identification based on artifactual +80â $\in D$ a modification at this site. Proteomics, 2011, 11, 829-842.	2.2	4
61	Liquid-like and solid-like motions in proteins. Journal of Molecular Liquids, 2002, 98-99, 383-400.	4.9	3
62	Identification and structural characterization of novel <i>O</i> ―and <i>N</i> â€glycoforms in the urine of a Schindler disease patient by Orbitrap mass spectrometry. Journal of Mass Spectrometry, 2015, 50, 1044-1056.	1.6	3
63	A natural diversity screen in <scp><i>Arabidopsis thaliana</i></scp> reveals determinants for <scp>HopZ1a</scp> recognition in the <scp>ZAR1â€ZED1</scp> immune complex. Plant, Cell and Environment, 2021, 44, 629-644.	5.7	3
64	The Design of New HIV-IN Tethered Bifunctional Inhibitors Using Multiple Microdomain Targeted Docking. Current Medicinal Chemistry, 2019, 26, 2574-2600.	2.4	3
65	Motions in native and denatured proteins. Physica B: Condensed Matter, 1997, 241-243, 1110-1114.	2.7	2
66	The Glycosylation of Tyrosinase in Melanoma Cells and the Effect on Antigen Presentation. Advances in Experimental Medicine and Biology, 2003, 535, 257-269.	1.6	2
67	Mass Spectrometry for Cancer Biomarkers. , 0, , .		2
68	Deep Learning in the Quest for Compound Nomination for Fighting COVID-19. Current Medicinal Chemistry, 2021, 28, 5699-5732.	2.4	2
69	Purification and partial characterization of a lectin from Datura innoxia seeds. Phytochemistry, 1993, 34, 343-348.	2.9	1
70	Abstract 2526: Tyrosine 656 in topoisomerase Il \hat{I}^2 is important for the catalytic activity. , 2011, , .		0